

Numerical Simulations of Constant-Volume Spray Combustion of n-Heptane with Chemical Kinetics

Jing Yang Tan¹, Hoon Kiat Ng^{1*}, Suyin Gan² and Fabrizio Bonatesta³

¹Department of Mechanical, Materials and Manufacturing Engineering, Jalan Broga, Semenyih – 43500, Selangor, Malaysia;

²Department of Chemical Engineering, The University of Nottingham Malaysia Campus, Jalan Broga, Semenyih – 43500, Selangor, Malaysia;

³Department of Mechanical Engineering and Mathematical Sciences, Oxford Brookes University, Wheatley Campus, Oxford OX33 1HX, United Kingdom; hoonkiatng@nottingham.edu.my

Abstract

Objectives: A reduced toluene reference fuel (TRF) mechanism of multi-component nature from the literature is utilized to simulate constant-volume spray combustion of n-heptane. The approach allows a preliminary assessment of fuel kinetic model and computational fluid dynamics (CFD) formulations in a simplified computational domain before integrating them in complex engine simulations.

Methods: The operating conditions vary in ambient densities between 14.8 kg/m³ and 30 kg/m³ with initial oxygen concentrations ranging from 10% to 21%. The CFD models are first calibrated to replicate spray penetration lengths of the non-reacting condition. The tuned numerical models are then applied to simulate the combustion and soot formation events of reacting sprays. The soot model employed is the multi-step Moss-Brookes model with updated oxidation models.

Findings: The relative errors for ignition delay and lift-off length predictions are within 35% and 22% respectively. Furthermore, simulated soot volume fraction contours agree qualitatively with the experimental soot clouds. Computed peak soot locations, however, are found to be further downstream axially as compared to the experimental results across all test cases.

Application: Good agreement with experimental spatial soot distributions allows the incorporation of both fuel and soot models in engine configurations.

Keywords: Chemical Kinetics, n-Heptane, Soot Model, Soot Volume Fraction

1. Introduction

While significant works have been devoted to improving performance of internal combustion engines, exhaust emissions remains one prominent issue hindering the current development. The emissions are mainly circumscribed by ultra-fine particulate matter (PM) which affects the respiratory health of adults severely¹. Consequently, implementation of stringent legislations drives major carmakers to seek for cost-effective control strategies to mitigate harmful emissions. Within this context, in-depth understanding of soot formation mechanisms is crucial to tackle the root of the problem.

The study of diesel soot has been ongoing for several decades until today. In addition, gasoline soot is receiving much attention currently due to the relatively recent identification of gasoline direct injection engines as an important source of anthropogenic PM. Often, Computational Fluid Dynamics (CFD) modelling serves to complement the engine studies utilizing advanced experimental and optical techniques. Successful numerical simulations depend on selection of accurate models to represent the in-cylinder events and precise descriptions of fuel chemical kinetics.

*Author for correspondence

In this study, the performance of a reduced Toluene Reference Fuel (TRF) mechanism, coupled with Polycyclic Aromatic Hydrocarbon (PAH), is evaluated within the constant-volume spray combustion environment. In particular, the application of multi-component mechanism incorporating cross-reactions between n-heptane and other fuel components is explored. Moreover, the inclusion of PAH chemistry provides the use of reliable soot precursor species for soot formation results. The test configurations allow validation of chemical kinetics of the model under engine-like operating conditions without complications induced by complex engine geometries. Furthermore, the applicability of CFD sub-models, particularly the multi-step soot model is examined. Therefore, the work serves as a preliminary assessment of fuel kinetics and soot model for subsequent combustion and emission modelling in engines.

2. Constant-Volume Spray Combustion Modelling

Experimental spray combustion of n-heptane fuel in a constant-volume combustion chamber (Spray H configurations) was performed by² the reference. The combustion vessel contains a cubical-shaped chamber with the characteristic dimension of 108 mm. The common-rail fuel injector is mounted in one side port with a metal insert, which forms the right wall of the combustion chamber. The ambient conditions in the present study include the non-reacting case without oxygen (O_2) and reacting cases with varying initial O_2 concentration levels at low and high ambient densities as tabulated in Table 1. The pressures lie within 40 to 50 bar for low ambient density cases and 80 to 90 bar in high ambient density conditions.

Table 1. Operating conditions of the constant-volume spray combustion experiments

T(K)	ρ (kg/m ³)	O_2 level (%)
1000	14.8	21, 15, 12, 10, 0 [#]
	30.0	15, 12, 10

[#] O_2 level of 0% indicates the non-reacting spray.

2.1 Numerical Formulations

The computational work is performed using an open source CFD code, Open FOAM version 2.0x. The combustion chamber is represented by a cylinder with an

axial length of 138 mm and a radial length of 54 mm in order to match the volume of experimental chamber. To reduce the computational time, an axisymmetric wedge, which is essentially a 4 degree sector of the cylindrical chamber, is modelled. The wedge possesses only a single layer of cells along its width, thus simplifying the chamber into a quasi-2D geometry. Spray combustion events of n-heptane are simulated within the wedge. The results are then validated against experimental measurements of Liquid Penetration Length (LPL), Vapour Penetration Length (VPL), Ignition Delay (ID), Lift-off Length (LOL) and Soot Volume Fraction (SVF).

The fuel kinetic model utilized is a reduced TRF model integrated with a sub-mechanism of PAH up to pyrene (A_4) developed by³ this reference. Consisting of 109 species among 543 reactions, the resulting fuel mechanism has been validated against experimental ID in shock tube, laminar flame speeds, species concentrations in premixed flames as well as homogeneous charge and direct injection compression ignition engine combustion data.

Coupled with chemical kinetics, appropriate CFD models are utilized to characterize the constant-volume spray combustion of n-heptane. Atomization is treated by injecting blobs, which have the same diameter as the nozzle exit. The injected blobs dissociate as they interact with the surrounding gas, thus producing a core region with relatively large droplets. The spray breakup is described by⁴, assuming that the contributing cause is interfacial forces of aerodynamic and surface forces. Droplet breakup occurs in two different modes, namely bag breakup and stripping breakup, depending on the criteria defined by both Weber and Reynolds numbers.

To account for turbulence induced, the standard k-epsilon model is used. The initial turbulent kinetic energy and dissipation rate are set to 0.735 m²/s² and 3.5 m²/s³ respectively. In addition, fuel evaporation is modelled through the Frossling correlations while the Ranz-Marshall model is implemented to compute droplet heat transfer with the surrounding gas phase. A dynamic drag model is utilized while droplet collision is neglected. The thermo physical model used calculates enthalpy for combustible mixtures based on sensible enthalpy or internal energy and compressibility.

In the present study, Moss-Brookes model is incorporated to simulate the associated soot formation and

oxidation processes of spray combustion. Purely empirical correlations are overly simplistic with limited applicability while detailed soot modelling is often obscured by the high computational cost. Therefore, the multi-step soot model employed is of semi-empirical nature and accounts for nucleation, surface growth, coagulation and oxidation⁵. Transport equations for normalized radical nuclei concentration and soot mass fraction are solved within the model. Subject to nucleation from the gas phase and coagulation in the free molecular regime, the instantaneous production rate of soot particles, $\frac{dN}{dt}$ is given in Equation (1).

$$\frac{dN}{dt} = C_\alpha N_A \left(\frac{X_{prec} P}{RT} \right)^l \exp\left(-\frac{T_\alpha}{T}\right) - C_\beta \left(\frac{24RT}{\rho_{soot} N_A} \right)^{\frac{1}{2}} d_p^{\frac{1}{2}} N^2 \quad (1)$$

Here, C_α , C_β and l are model constants. N_A denotes the Avogadro number (6.022045×10^{26} kmol⁻¹). X_{prec} is the mole fraction of A_4 acting as the soot precursor. The soot density, ρ_{soot} is assumed to be 2000 kg/m³. d_p is the mean diameter of a soot particle. On the other hand, the source term for soot mass concentration is represented by the expression shown in Equation (2), taking into account the phases of nucleation, surface growth and oxidation.

$$\begin{aligned} \frac{dM}{dt} = & M_P C_\alpha \left(\frac{X_{prec} P}{RT} \right)^l \exp\left(-\frac{T_\alpha}{T}\right) + C_\gamma \left(\frac{X_{sgs} P}{RT} \right)^m \exp\left(-\frac{T_\gamma}{T}\right) \left[(\pi N)^{\frac{1}{2}} \left(\frac{6M}{\rho_{soot}} \right)^{\frac{2}{3}} \right]^n \\ & - C_{oxid,1} C_{\omega,1} n_{coll} \left(\frac{X_{OH} P}{RT} \right)^{\frac{1}{2}} \sqrt{T} (\pi N)^{\frac{1}{2}} \left(\frac{6M}{\rho_{soot}} \right)^{\frac{2}{3}} \\ & - C_{oxid,2} C_{\omega,2} n_{coll} \left(\frac{X_{O_2} P}{RT} \right)^{\frac{1}{2}} \exp\left(-\frac{T_{w,2}}{T}\right) \sqrt{T} (\pi N)^{\frac{1}{2}} \left(\frac{6M}{\rho_{soot}} \right)^{\frac{2}{3}} \end{aligned} \quad (2)$$

Here, C_γ , C_{oxid} , $C_{\omega,1}$, $C_{\omega,2}$, m and n are model constants. M_P refers to the mass of an incipient soot particle, comprising 100 carbon atoms with a constant value of 1200 kg/kmol. X_{sgs} , X_{OH} and X_{O_2} represent the mole fractions of participating surface growth specie, acetylene (C₂H₂), hydroxyl (OH) radical and molecular O₂, respectively. To improve calculations of soot oxidation in the Moss-Brookes model, oxidation by OH radicals is adapted according to the model proposed by⁶ whereas oxidation by O₂ follows the model formulated by⁷.

3. Results and Discussion

3.1 Non-reacting Spray

The CFD models are first calibrated based on experimental findings of the non-reacting condition to

identify the optimum numerical settings for subsequent reacting conditions. The computational domain with smallest cell sizes of 0.5 mm axially and 0.25 mm radially is found to achieve mesh independence. Furthermore, time step size of 0.2 μs is used while the number of parcels is fixed at 100000 for both non-reacting and reacting spray simulations. In order to emulate the vapor penetration profile, the time factor constant, C_s within model⁴ is modified to be 11.5. Meanwhile, adjusting the model constant, $C_{1\epsilon}$ of the standard k-epsilon model to 1.53 (approximation for round jets⁸) provides good agreement to experimentally measured LPL. The resulting predicted LPL and VPL profiles are illustrated in Figure 1 along with the experimental data.

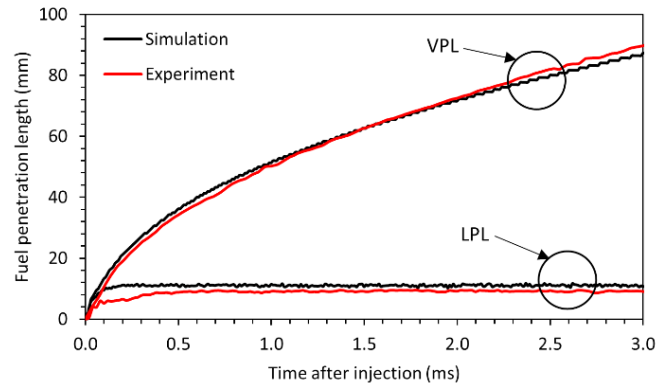


Figure 1. Comparisons of simulated and measured LPL and VPL for the non-reacting condition.

3.2 Reacting Sprays

Figure 2 displays the comparisons of simulated ID and LOL against their experimental measurements at different initial O₂ concentrations for low ($\rho = 14.8$ kg/m³) and high ($\rho = 30$ kg/m³) ambient density conditions. As observed, the model reproduces measured ID and LOL across varying O₂ concentrations at both ambient densities. The maximum relative errors for ID and LOL predictions are 35% and 22% respectively for all the cases. The trends of decreasing ID and LOL with increasing O₂ content are accurately captured. Higher levels of O₂ promote favourable combustion conditions, thus lowering the time needed for fuel ignition and combustion.

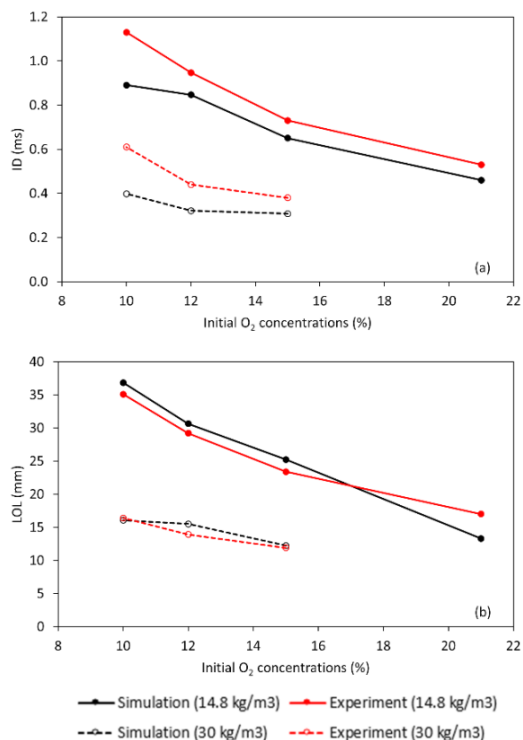


Figure 2. Comparisons of simulated and measured (a) ID and (b) LOL at different initial O₂ concentrations.

Simulated spatial soot evolutions are represented by SVF contours. For brevity, only test cases with initial O₂ level of 15% are illustrated in Figure 3 along with the experimental results in the quasi-steady state. Generally, shapes and contours of soot clouds are replicated by the model reasonably for all reacting sprays. From Figure 3, computed peak soot locations at 15% O₂ level are found approximately 10 to 15 mm further away from the injector nozzle as compared to the experimental locations. The overestimation of peak soot locations is consistent across other test cases with varied initial O₂ concentrations.

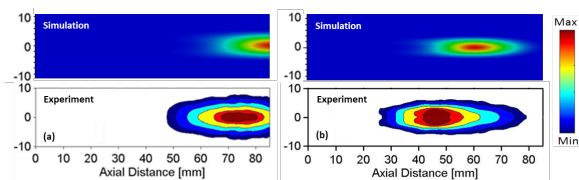


Figure 3. Comparisons of simulated and measured soot contours at initial O₂ concentration of 15% for (a) low ($\rho = 14.8 \text{ kg/m}^3$) and (b) high ($\rho = 30 \text{ kg/m}^3$) ambient density conditions.

Nonetheless, the model captures the variation of spatial soot distributions with respect to the change in O₂ levels. Test cases with varied initial concentrations of O₂ correspond to engine-like operating conditions with different rates of exhaust gas recirculation (EGR). With decreasing O₂ content (higher ERG rate), it is found that soot clouds are formed at longer axial distances from the injector position at a given ambient density. The downstream shift of soot clouds is likely caused by the lowered rate of air entrainment into the fuel jet, when the ambient O₂ concentrations are reduced⁹.

Meanwhile, the effect of ambient density on region of soot formation is obvious as exemplified in Figure 3. For a similar initial O₂ content, soot regions are located closer to the injector nozzle at higher ambient density conditions due to the higher ambient pressure. The observation is corroborated by shorter LOL displayed in Figure 2(b) for ambient density of 30 kg/m³. The trend is fairly well captured by the model. It is noteworthy that the comparisons of SVF profiles in the present study are qualitative in nature as model constants in the soot model are retained at their default values.

4. Conclusion

CFD simulations of spray combustion of n-heptane within a constant-volume environment are performed using a reduced TRF mechanism integrated with PAH chemistry. The multi-step Moss-Brookes soot model is coupled with the spray combustion solver to describe the soot formation and oxidation processes. Reasonable agreement of LPL, VPL, ID and LOL with experimental measurements across the range of operating conditions implies that both fuel-air mixing and combustion characteristics are emulated. The trends of longer ID and higher LOL with decreasing O₂ level are correctly reproduced by the model. Additionally, shapes, contours and distributions of simulated soot clouds in all reacting conditions resemble their experimental counterparts. Computed peak soot locations from the injector position are however, slightly overestimated. It is observed that at a similar concentration of O₂, soot clouds are formed further away from the injector axially when the ambient density decreases. On the other hand, the locations of soot clouds are closer to the injector with increasing O₂ level at a given ambient density. Overall, variation of spatial soot dis-

tributions with respect to changes in O_2 content and ambient density are captured by the model. Hence, the fuel kinetic model, along with the CFD formulations, can subsequently be adapted to simulate complex in-cylinder events of engines.

5. Acknowledgement

The Ministry of Higher Education (MOHE) Malaysia is gratefully acknowledged for the financial support towards the study under the Fundamental Research Grant Scheme (FRGS), FRGS/1/2014/TK01/UNIM/01/1.

6. References

1. Penttinen P, Timonen KL, Tiittanen P, Mirme A, Ruuskanen J, Pekkanen J. Ultrafine particles in urban air and respiratory health among adult asthmatics. *European Respiratory Journal*. 2001 Mar; 17(3):428–35.
2. Sandia National Laboratories. Combustion vessel geometry: 2009 to present. Available from: Crossref. Date accessed: 12/09/2016.
3. Wang H, Yao M, Yue Z, Jia M, Reitz RD. A reduced toluene reference fuel chemical kinetic mechanism for combustion and polycyclic-aromatic hydrocarbon predictions. *Combustion and Flame*. 2015;162(6):2390–404.
4. Reitz RD, Diwakar R. Effect of drop breakup on fuel sprays. SAE Technical Paper. Available from: Crossref. Date accessed: 1986.
5. Brookes S, Moss J. Predictions of soot and thermal radiation properties in confined turbulent jet diffusion flames. *Combustion and Flame*. 1999 Mar;116(4):486–503.
6. Fenimore CP, Jones GW. Oxidation of soot by hydroxyl radicals. *Journal of Physical Chemistry*. 1967 Feb;71(3):593–7.
7. Lee KB, Thring MW, Beér JM. On the rate of combustion of soot in a laminar soot flame. *Combustion and Flame*. 1962; 6:137–45.
8. Novella R, García A, Pastor JM, Domenech V. The role of detailed chemical kinetics on CFD diesel spray ignition and combustion modelling, *Mathematical and Computer Modelling*. 2011 Oct;54(7-8):1706–19.
9. Idicheria CA, Pickett LM. Soot formation in diesel combustion under high-EGR conditions. SAE Technical Paper. 2005.